Early-time dynamics of Bose gases quenched into the strongly interacting regime

Alberto Muñoz de las Heras[1, *]

[1] *Departamento de Física Teórica de la Materia Condensada & Condensed Matter Physics Center (IFIMAC), Universidad Autónoma de Madrid, Madrid 28049, Spain*

(Dated: September 2, 2018)

Ultracold atomic Bose-Einstein condensates with tunable interactions have been proved a rich and very active field of research. The experimental access to the strongly interacting regime has been limited by the gas short lifetime due to three-body recombination processes. However, recent experiments [1, 2] have shown that after a sudden quench to unitarity, where the interatomic scattering length $a \to \infty$, two-body lossless dynamics develops faster than three-body processes, allowing the gas to attain a degenerate steady state. Furthermore, very recently [3] it has been possible to isolate the effects of the early-time lossless postquench dynamics, demonstrating the emergence of a universal prethermal steady state. Here, by making use of a time-dependent Nozières-Saint James variational formalism, that takes into account excitations out of the condensate in pairs only, we numerically study the early-time dynamics of a degenerate Bose gas after quenches to several values of a. We characterise the coherent oscillations between atomic and molecular states as function of the final scattering length of the gas, showing that after the quench the oscillatory behaviour becomes negligible as we consider a final a in the weakly interacting regime, while for large enough a it exhibits a crossover indicating the appearance of the unitary regime. For the largest scattering lengths we can numerically simulate, we find a universal scaling behaviour of the typical raising time of the momentum distribution in agreement with [3]. Finally, we discuss some preliminary results on possible future work.

I. INTRODUCTION

In the last decades ultracold atomic gases have succesfully emerged as a platform for the study of many-body quantum physics out of equilibrium. In particular, the possibility to dynamically change the effective interatomic interaction (a process known as quench) by means of Feshbach resonances has open the door to investigate the unitary regime, where interactions are as strong as allowed by quantum mechanics and new forms of universality are expected.

At low energies two-body scattering is described by an s-wave scattering length a that can be controlled by an external magnetic field taking advantage of Feshbach resonances [4]. In particular, the unitary regime, where $a \to \infty$, has attracted a growing interest in the last years. In this situation, even though Efimov physics was susceptible to induce non-universality, the dynamics has been consistent with the average interparticle distance $n^{-1/3}$ (written in terms of the gas density n) being the only relevant length scale [1], therefore showing universality in units of the Fermi momentum $k_n = (6\pi^2 n)^{1/3}$, energy $\epsilon_n = k_n^2/(2m)$ (where m is the mass of one atom) and time $t_n = 1/\epsilon_n$ (henceforth we fix $\hbar = 1$). This regime has been intensively studied in the case of clouds of fermionic atoms [5, 6], where Pauli exclusion principle prevents three-body recombination, which is the responsible of the decay of the gas to its truly equilibrium solid state. However, this statistical blockade is not present in the case of Bose gases, where the three-body recombination rate scales as $n^2 a^4$, and therefore in a unitary Bose-Einstein condensate (BEC) losses were expected to dominate.

However, it was found [1] that after a sudden quench of the interaction to the unitary regime, the timescale for three-body losses is much larger than that of lossless dynamics, allowing the momentum distribution to reach a steady-state before three-body recombinations take over the gas. Futhermore, it was measured [7] that after a quench to unitarity there is an early time window where the three-body contact C_3 (which is a measure of the strength of short-range, three-body correlations) remains negligible. These surprising results showed that one path to study the unitary Bose gas is to perform the measurements dynamically after a rapid quench of the interaction.

More recently, Eigen et al. [3] measured the population of individual states with a certain momentum k as a function of time in a homogenous degenerate Bose gas quenched to unitarity in an optical-box trap. The dynamics is first governed by lossless, two-body processes and the states evolve towards a prethermal steady state with a population $\bar{n}_k$ in a timescale τ_{grow}, that is later destroyed by long-time heating due to three-body recombinations. When plotting τ_{grow} as function of k, they found a universal prethermal behaviour, with all the dynamics being consistent with k_n and t_n as the only characteristic momentum and time scales. A more striking result is that $\bar{n}_k$ does not decay as $1/k^4$, as one would expect for a quantum gas governed by short-range, two-body interactions [8], but rather decays exponentially with k.

In this Master's thesis, by making use of Nozières-Saint James variational formalism [9], that takes into account two-body scattering processes only, we study the early-time dynamics of homogeneous, degenerate Bose gases

* alberto.munnozd@estudiante.uam.es

quenched to different interaction strengths, ranging from the weakly to the strongly interacting regime. We describe the short-range, 2-body interactions of the gas with a δ-like pseudopotential characterised by an s-wave scattering length, that is renormalised and thus accounts for the molecular bound state in the repulsive side of the resonance.

As found by [10], this molecular bound state plays a crucial role in the post-quench dynamics, producing coherent oscillations in the number of particles excited out of the condensate n_{ex} and Tan's contact $C(t)$. We characterise, as a function of the gas final scattering length, the behaviour of these oscillations and our results anticipate the crossover to the unitary regime. We also find an universal scaling behaviour of the typical raising time τ_{grow} of the population of individual k states for long enough interactions, in agreement with [3]. However, our model is not able to reproduce the exponential decay of the steady state population $\bar{n}_k$ as function of k, but rather displays the typical $1/k^4$ behaviour of quantum gases described by a two-body, s-wave contact interaction [8].

II. MODEL

We start considering the Hamiltonian describing a homogeneous gas of N interacting bosons in a three-dimensional (3D) volume V

$$\hat{H} = \sum_{\mathbf{k}} \epsilon_{\mathbf{k}} \hat{a}^\dagger_{\mathbf{k}} \hat{a}_{\mathbf{k}} + \frac{U_\Lambda}{2V} \sum_{\mathbf{k}_1,\mathbf{k}_2,\mathbf{q}} \hat{a}^\dagger_{\mathbf{k}_1+\mathbf{q}} \hat{a}^\dagger_{\mathbf{k}_2-\mathbf{q}} \hat{a}_{\mathbf{k}_1} \hat{a}_{\mathbf{k}_2} \ , \quad \text{(II.1)}$$

where $\hat{a}^\dagger_{\mathbf{k}}$ ($\hat{a}_{\mathbf{k}}$) creates (annihilates) a boson with momentum $\mathbf{k}$ and mass m ($\epsilon_{\mathbf{k}} = k^2/2m$). Close to a Feshbach resonance, atom interactions can be modelled via a short-range psudopotential which, in momentum space, is constant with strength U_Λ up to a momentum cutoff Λ. The coupling constant and cutoff are related to the s-wave scattering length a through the T-matrix renormalization process [4, 11]:

$$\frac{m}{4\pi a} = \frac{1}{U_\Lambda} + \frac{1}{V} \sum_{\mathbf{k}}^{k<\Lambda} \frac{1}{2\epsilon_{\mathbf{k}}} = \frac{1}{U_\Lambda} + \frac{m\Lambda}{2\pi^2} \ . \quad \text{(II.2)}$$

The cutoff Λ represents the inverse range of the interaction potential. In the $\Lambda \to \infty$ limit, the contact potential admits, on the repulsive side of the resonance $a > 0$, a single molecular bound state with energy [10, 12]

$$E_{\rm B} = -\frac{1}{ma^2} \ . \quad \text{(II.3)}$$

In order to separate the contribution of the condensed state $\mathbf{k} = \mathbf{0}$ from the one of the excited states $\mathbf{k} \neq \mathbf{0}$, it is useful to rewrite the Hamiltonian (II.1) by substituting $\hat{a}_{\mathbf{k}} \to \hat{a}_0 \delta_{\mathbf{k},\mathbf{0}} + \hat{a}_{\mathbf{k}\neq\mathbf{0}}$ (we henceforth use the notation $\hat{a}_{\mathbf{k}}$ for $\hat{a}_{\mathbf{k}\neq\mathbf{0}}$). One obtains

$$\hat{H} = \sum_{\mathbf{k}} \epsilon_{\mathbf{k}} \hat{a}^\dagger_{\mathbf{k}} \hat{a}_{\mathbf{k}} + \frac{U_\Lambda}{2V} \hat{a}^\dagger_0 \hat{a}^\dagger_0 \hat{a}_0 \hat{a}_0 + \hat{H}_2 + \hat{H}_3 + \hat{H}_4 \quad \text{(II.4)}$$

$$\hat{H}_2 = \frac{U_\Lambda}{2V} \sum_{\mathbf{k}} \left(\hat{a}^\dagger_{\mathbf{k}} \hat{a}^\dagger_{-\mathbf{k}} \hat{a}_0 \hat{a}_0 + 2\hat{a}^\dagger_{\mathbf{k}} \hat{a}_{\mathbf{k}} \hat{a}^\dagger_0 \hat{a}_0 + \text{h.c.} \right) \quad \text{(II.5)}$$

$$\hat{H}_3 = \frac{U_\Lambda}{V} \sum_{\mathbf{k},\mathbf{q}} \left(\hat{a}^\dagger_{\mathbf{k}-\mathbf{q}} \hat{a}^\dagger_{\mathbf{q}} \hat{a}_{\mathbf{k}} \hat{a}_0 + \text{h.c.} \right) \quad \text{(II.6)}$$

$$\hat{H}_4 = \frac{U_\Lambda}{2V} \sum_{\mathbf{k}_1,\mathbf{k}_2,\mathbf{q}} \hat{a}^\dagger_{\mathbf{k}_1+\mathbf{q}} \hat{a}^\dagger_{\mathbf{k}_2-\mathbf{q}} \hat{a}_{\mathbf{k}_1} \hat{a}_{\mathbf{k}_2} \ . \quad \text{(II.7)}$$

At zero temperature, we describe the early time dynamics of the gas after a quench from an initial scattering length a_i to final value a_f via the time-dependent generalisation of the Nozières-Saint James variational Ansatz [9, 13]:

$$|\psi(t)\rangle = \frac{1}{\mathcal{N}(t)} \exp\left[\sqrt{V} c_0(t) \hat{a}^\dagger_0 + \sum_{\mathbf{k}}^{-} \frac{g_{\mathbf{k}}(t)}{2} \hat{a}^\dagger_{\mathbf{k}} \hat{a}^\dagger_{-\mathbf{k}} \right] |0\rangle \ , \quad \text{(II.8)}$$

where $g_{-\mathbf{k}}(t) = g_{\mathbf{k}}(t)$. The factor $1/2$ in the momentum sum avoids double-counting and we use the notation $\bar{\sum}_{\mathbf{k}} = \sum_{\mathbf{k}\neq\mathbf{0}}^{k<\Lambda}$. The normalisation constant $\mathcal{N}(t)$ ensures that $\langle\psi(t)|\psi(t)\rangle = 1$.

The complex variational parameters $c_0(t)$ and $g_{\mathbf{k}}(t)$ are related to the momentum occupation numbers,

$$N_0(t) = \langle \hat{a}^\dagger_0 \hat{a}_0 \rangle = V |c_0(t)|^2 \quad \text{(II.9)}$$

$$N_{\mathbf{k}}(t) = \langle \hat{a}^\dagger_{\mathbf{k}} \hat{a}_{\mathbf{k}} \rangle = \frac{|g_{\mathbf{k}}(t)|^2}{1 - |g_{\mathbf{k}}(t)|^2} \ , \quad \text{(II.10)}$$

and to the pairing term:

$$x_{\mathbf{k}}(t) = \langle \hat{a}_{\mathbf{k}} \hat{a}_{-\mathbf{k}} \rangle = \frac{g_{\mathbf{k}}(t)}{1 - |g_{\mathbf{k}}(t)|^2} \ , \quad \text{(II.11)}$$

where $\langle \dots \rangle = \langle\psi(t)| \dots |\psi(t)\rangle$. Note that $N_{\mathbf{k}}(t)$ and $x_{\mathbf{k}}(t)$ are not independent functions, rather are constrained by $|x_{\mathbf{k}}(t)|^2 = N_{\mathbf{k}}(t)\,[N_{\mathbf{k}}(t) + 1]$. The same Ansatz (II.8) has already been considered by [10, 14] to describe the quench dynamics of a Bose gas into the strongly interacting regime. $|\psi(t)\rangle$ describes the $\mathbf{k} = \mathbf{0}$ condensed state as a coherent state, while particles at finite momentum $\mathbf{k} \neq \mathbf{0}$ are excited out of the condensate in pairs only. For shallow quenches ($n a_f^3 \ll 1$), the condensate depletion is small, $|c_0(t)|^2 \simeq n$ and (II.8) is a controlled approximation at an early stage of the dynamics, when Beliaev-Landau scattering processes involving three particles can be safely neglected [15]. In this limit, one can neglect the contributions of $\hat{H}_3$ and $\hat{H}_4$ to the Hamiltonian and thus the dynamics becomes integrable (see App. A), recovering the results obtained by Refs. [16, 17] in within a time-dependent Bogoliubov approximation.

We use the Ansatz (II.8) to study the crossover of

the early-time dynamics from shallow $na_f^3 \ll 1$ to deep $na_f^3 \gg 1$ quenches. The fact that the dynamics of the condensate depletion cannot now be neglected is included in the time dependence of the variational parameter $c_0(t)$, in a similar fashion to the self-consistent Bogoliubov approximation considered by [18].

Further, as explained later, we include the contribution of $\langle \hat{H}_4 \rangle$, thus allowing correlations between non-condensed atoms. However, as $\langle \hat{H}_3 \rangle = 0$, the Ansatz for $|\psi(t)\rangle$ does not admit neither Beliaev decay nor Landau damping terms that may be responsible for the loss of atom-molecule coherence.

One expects that, by increasing the value of the final scattering length towards unitarity, the separation of time scales predicted by [15] between a short-time dynamics dominated by pair-wise excitations and a longer-time dynamics requiring the inclusion of higher-order exciation terms will get reduced. However, the generalisation of (II.8) to include three-particle processes is beyond the scope of this work and will be the subject of future studies.

A. Equations of motion

As in [10, 14], the equations of motion for the variational parameters $c_0(t)$ and $g_{\mathbf{k}}(t)$ can be derived from the Euler-Lagrange equations [10, 19]:

$$\frac{d}{dt}\frac{\partial \mathcal{L}}{\partial \dot{c}_0^*} = \frac{\partial \mathcal{L}}{\partial c_0^*} \qquad \frac{d}{dt}\frac{\delta \mathcal{L}}{\delta \dot{g}_{\mathbf{k}}^*} = \frac{\delta \mathcal{L}}{\delta g_{\mathbf{k}}^*} \ .$$

where

$$\mathcal{L} = \frac{i}{2}\left[\langle\psi(t)|\dot{\psi}(t)\rangle - \langle\dot{\psi}(t)|\psi(t)\rangle\right] - \langle \hat{H}\rangle \ .$$

When evaluating the contributions to $\langle \hat{H}\rangle$, we have that $\langle \hat{H}_3\rangle = 0$ while

$$\langle \hat{H}_4\rangle = \frac{U_\Lambda}{2V}\bar{\sum_{\mathbf{k},\mathbf{q}}}\left[2N_{\mathbf{k}}(t)N_{\mathbf{q}}(t) + x_{\mathbf{k}}(t)x_{\mathbf{q}}^*(t)\right] \ . \quad \text{(II.12)}$$

Differently from [18], we retain the anomalous expectation values $x_{\mathbf{k}}$ in $\langle \hat{H}_4\rangle$, that lead to coherent, virtual transitions of pairs of atoms back and forth to a molecular condensate, with the energy of two bound atoms given by (II.3). Operating, one arrives to the following equations of motion:

$$i\dot{c}_0 = U_\Lambda c_0 n + \frac{U_\Lambda}{V}\bar{\sum_{\mathbf{k}}}\frac{c_0|g_{\mathbf{k}}|^2 + c_0^* g_{\mathbf{k}}}{1-|g_{\mathbf{k}}|^2} \quad \text{(II.13)}$$

$$i\dot{g}_{\mathbf{k}} = 2\left[\epsilon_{\mathbf{k}} + U_\Lambda n\right]g_{\mathbf{k}} + U_\Lambda\left(2|c_0|^2 g_{\mathbf{k}} + g_{\mathbf{k}}^2 c_0^{*2} + c_0^2\right) + \frac{U_\Lambda}{V}\bar{\sum_{\mathbf{q}}}\frac{2g_{\mathbf{k}}|g_{\mathbf{q}}|^2 + g_{\mathbf{k}}^2 g_{\mathbf{q}}^* + g_{\mathbf{q}}}{1-|g_{\mathbf{q}}|^2} \ , \quad \text{(II.14)}$$

$n = 10^{12} cm^{-3}$	na^3	$\xi(\mu m)$	$\tau(ms)$	$\lvert E_B\rvert^{-1}(\mu s)$
$a = 100a_0$	$1.48 \cdot 10^{-7}$	2.74	20.1	$3.74 \cdot 10^{-2}$
$a = 1000a_0$	$1.48 \cdot 10^{-4}$	0.867	2.00	3.74
$a = 60000a_0$	32.0	0.112	$3.35 \cdot 10^{-2}$	$1.35 \cdot 10^4$

TABLE I. Values of the natural system lengthscales and timescales, as well as of the interaction strength parameter na^3, for different scattering lengths, in a gas of ^{85}Rb with density $n = 10^{12} cm^{-3}$ (N.B. that $k_n^{-1} = 0.257 \mu m$ and $\epsilon_n^{-1} = 0.176 ms$ independently of the scattering length).

that have to be solved for a set of initial conditions $c_0(0)$ and $g_{\mathbf{k}}(0)$. Note that the total density

$$n = n_0(t) + n_{ex}(t) = |c_0(t)|^2 + \frac{1}{V}\bar{\sum_{\mathbf{k}}} N_{\mathbf{k}}(t) \ , \quad \text{(II.15)}$$

written as the sum of the density of condensed (n_0) and non-condensed (n_{ex}) atoms, is conserved during the dynamics.

For instantaneous quenches $a_i \to a_f$, the equations of motion (II.13) and (II.14) have to be solved for $U_\Lambda = U_{\Lambda,f} = (1 - 2a_f\Lambda/\pi)^{-1} 4\pi a_f/m$, while the initial conditions can be found by minimising $\langle\psi|\hat{H} - \mu\hat{N}|\psi\rangle$ (for $U_\Lambda = U_{\Lambda,i}$) at a fixed number of particles with respect to time-independent variational parameters $c_0(0)$ and $g_{\mathbf{k}}(0)$. For example, for an initial weakly interacting gas $na_i^3 \ll 1$, one has that

$$|c_0(0)|^2 = n\left(1 - \frac{8}{3\sqrt{\pi}}\sqrt{na_i^3}\right) \simeq n \quad \text{(II.16)}$$

$$g_{\mathbf{k}}(0) = \frac{\sqrt{\epsilon_{\mathbf{k}}(\epsilon_{\mathbf{k}} + 2U_i n)} - (\epsilon_{\mathbf{k}} + nU_i)}{nU_i} \ , \quad \text{(II.17)}$$

where $U_i = 4\pi a_i/m$. For shallow quenches, the dynamics is integrable and, as shown in App. A, Eqs. (II.13) and (II.14) can be solved exactly. We instead want to describe the evolution of the system dynamics from shallow to deep quenches and to this end we numerically integrate the dynamics.

B. Parameters

Here we review the relevant system parameters in the different regimes of interaction strength. For a weakly interacting gas $na_f^3 \ll 1$, the effect of the resonance is negligible and the quasiparticle dynamics is governed by the healing length and mean-field time (i.e., it can be described with Bogoliubov theory) [20]:

$$\xi = \frac{1}{\sqrt{8\pi a n}} \qquad \tau = \frac{m}{4\pi a n} \ . \quad \text{(II.18)}$$

For larger scattering lengths the molecular bound state energy E_{B} becomes relevant, and towards unitarity $a \to \infty$, k_n and ϵ_n are expected to be the only physically meaningful scales remaining. Values of these quantities

for a gas of ^{85}Rb with density $n = 10^{12} cm^{-3}$ calculated for three scattering lengths representative of the above mentioned regimes are shown in Table I.

III. RESULTS

We describe the early-time quench dynamics of a Bose-Einstein condensate at zero temperature as a function of the final scattering length a_f all the way towards unitarity. To this end, we numerically solve the equations of motion (II.13) and (II.14) for the specific case of instantaneous quenches from a non-interacting gas ($a_i = 0$, $c_0(0) = \sqrt{n}$ and $g_{\mathbf{k}}(0) = 0$) to a generic value of a_f. We assume spherical symmetry for $g_{\mathbf{k}}(t) = g_k(t)$, use a Gauss-Legendre quadrature and integrate the equations of motion using a 4^{th}-order Runge-Kutta routine. The dynamics has thefore two regularisation parameters, namely the number of points M on the Gauss-Legendre momentum grid and the momentum cutoff Λ. As explained in App. B, we have checked the convergence of our results with respect to both parameters and extrapolated the numerics to $M \to \infty$ and $\Lambda \to \infty$.

A. Non-condensed fraction

We plot in Fig. 1 the density of particles in excited states (II.15) as a function of time and for different values of the final scattering length a_f after an instantaneous quench from a non-interacting gas $a_i = 0$. We rescale both the non-condensed density $n_{ex}(t)$ and the time t by different parameters depending on the range of the final scattering length we consider a_f. In particular, in the weakly interacting regime (panel (a)) we rescale density and time using the healing length ξ and mean-field time τ (II.18). In this regime, the results obtained within a time-dependent Bogoliubov approximation (see App. A) are in fact universal in these units and one can easily solve Eq. (A.7) for the early-time dynamics:

$$n_{ex}^{Bog}(t)\xi^3 \underset{t \ll \tau}{\simeq} \frac{1}{4\pi^{3/2}} \sqrt{\frac{t}{\tau}} \,. \tag{III.1}$$

As Fig. 1(a) shows, this "universal" (i.e., independent on the value of the final scattering length a_f) behaviour of $n_{ex}^{Bog}(t)$ in units of ξ and τ in the weakly interacting regime is only weakly modified by the inclusion of both the dynamics of the condesate $c_0(t)$ and the correlations between non-condensed atoms, which our equations of motion (II.13) and II.14 introduce. In particular, our description takes into account the presence of the molecular bound state in the repulsive side of the Feshbach resonance, and therefore coherent oscillations appear in the density of excited particles due to a virtual transfer of pairs of atoms to it. Because the molecular binding energy E_{B} (II.3) decreases by increasing a_f, the period of oscilations increases in these units. Also note that the mean condensate depletion is always above the prediction obtained within the Bogoliubov approximation and this discrepancy increases by increasing a_f.

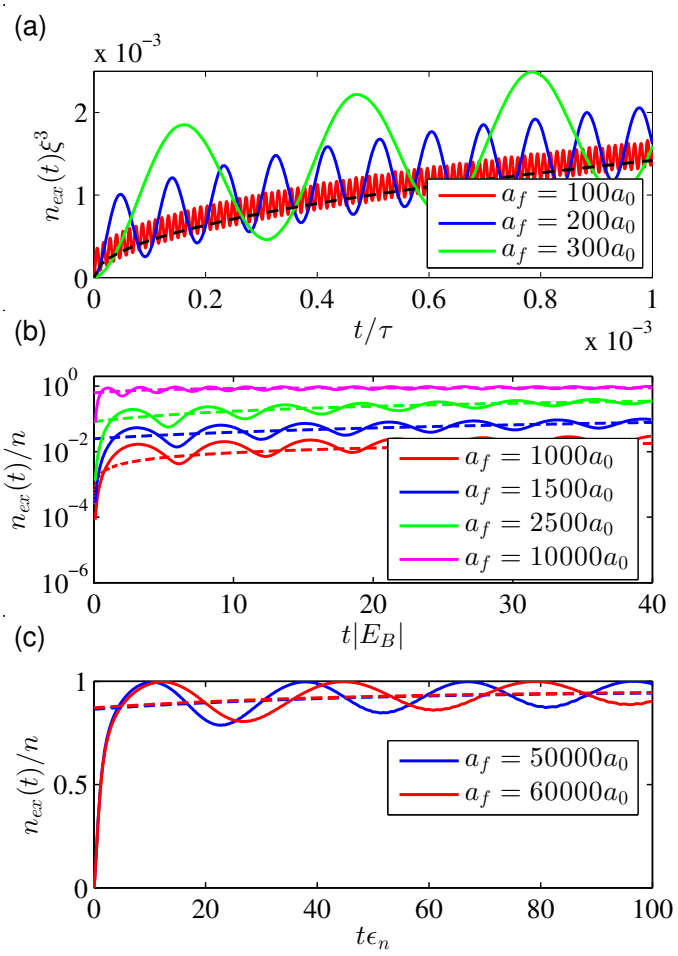

FIG. 1. Non-condensed density $n_{ex}(t)$ as a function of time and for different values of the final scattering length a_f after an instantaneous quench from a non-interacting gas $a_i = 0$. In all panels, solid lines are the results of the numerical integration of the equations of motion (II.13) and (II.14). In panel (a), the dashed line corresponds to the result obtained within the Bogoliubov approximation (A.7) [16], while in both panels (b) and (c), the dashed lines are fittings of the longer time-scale dynamics, from which we extract the steady-state mean value $\bar{n}_{ex}$ reported in Fig. 2 (except for $a_f = 1000a_0$, in which the dashed line is the prediction of Bogoliubov theory). Density is fixed at $n = 10^{12} cm^{-3}$.

Fig. 1(b) shows the time evolution of n_{ex}/n for larger final scattering lengths a_f, with the time rescaled in units of $|E_B|$. As will be shown later, the period of oscillations in quenches to $a_f \lesssim 1000a_0$ has an universal value of $T = 2\pi/|E_B|$, while for $a_f \gtrsim 1000a_0$ it starts decreasing.

The dynamics of n_{ex}/n for even larger a_f can be seen in Fig. 1(c), with time rescaled in units of ϵ_n. As discussed in App. B, the dynamics convergence slows critically down when increasing the value of a_f and $a_f = 60000a_0$ is the largest we can consider. In this regime, the av-

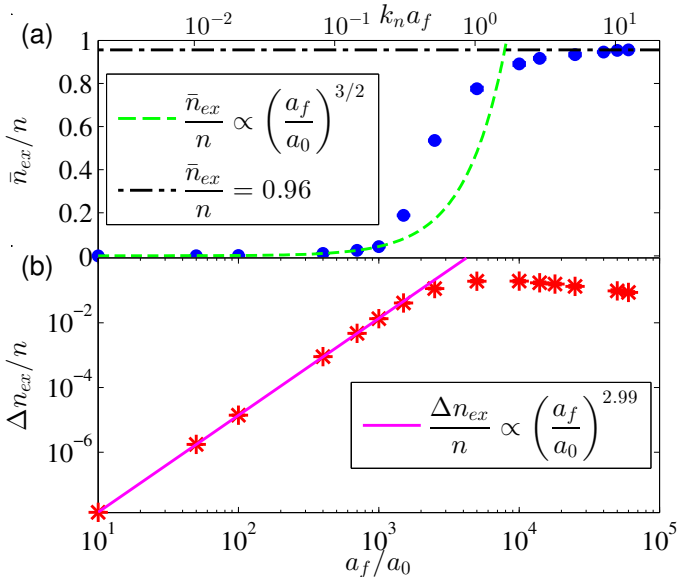

FIG. 2. **(a)** Steady-state mean value of the non-condensed density at large times $\bar{n}_{ex}$ as a function of a_f in the crossover from shallow ($na_f^3 \ll 1$) to deep ($na_f^3 \gg 1$) quenches. The dashed green line is the steady-state value within Bogoliubov theory (see (III.4)), while the black dot-dashed line marks the largest steady-state condensate deplition obtained for the largest a_f considered. Density is fixed at $n = 10^{12} cm^{-3}$. **(b)** Amplitude of the oscillations in the non-condensed fraction $\Delta n_{ex}/n$ as function of a_f. For $a_f \lesssim 1000a_0$ the values are very well adjusted to a cubic fit.

erage of the oscillations slowly approaches $n_{ex}/n = 1$, although this value is never reached in the maxima. In fact, Fig. 2(a) shows the large-time steady state reached by the average of the maxima and minima of the oscillations in n_{ex}/n as function of the final scattering length of the quench a_f, named $\bar{n}_{ex}/n$. For $a_f > 1000a_0$, the results plotted are obtained extrapolating to $t \to \infty$ the values of the average between consecutive maxima and minima using a fit of the shape $f(x) = a + be^{cx}$ (see App. C). The corresponding errors are given by the fit uncertainty. For $a_f \leq 1000a_0$, we would need to calculate the average of the oscillations for larger times in order to apply the fit. Therefore, in this range of scattering lengths Bogoliubov approximation has been used to obtain an order of magnitude estimation of the average of the oscillations. The errors in the case are estimated as a 20% of the amplitude of the oscillations. The non-condensed fraction in Bogoliubov approximation can be calculated from (A.7), which for $t \ll \tau$ and $t \gg \tau$ reduces respectively to

$$n_{ex}(t)\xi^3 = \frac{1}{4\pi^{3/2}}\sqrt{\frac{t}{\tau}}\,, \tag{III.2}$$

$$n_{ex}(t)\xi^3 = \frac{1}{\sqrt{2^7}\pi}\left(1 - e^{-4t/\tau}\right)\,. \tag{III.3}$$

This latter expression can also be written (II.18) as

$$\frac{n_{ex}}{n} = \frac{(8\pi a n^{1/3})^{3/2}}{\sqrt{2^7}\pi}\left(1 - e^{-4t/\tau}\right)\,. \tag{III.4}$$

In general, the average of the oscillations increases as a_f increases, slowly approaching $n_{ex}/n = 1$ for large enough scattering lengths.

In [18] $n_{ex}(t \to \infty)$ is studied for sudden quenches from $k_n a_i = 0.01$ (i.e. $a_i \simeq 50a_0$ in a gas of density $n = 10^{12} cm^{-3}$) to several values of a_f, and we see a good agreement between our variational results and their self-consistent dynamic field theory. In fact, with both formalisms the system seems to remain in the superfluid phase for an arbitrarily large final scattering length. For $k_n a_f \lesssim 0.1$ (i.e. $a_f \lesssim 500a_0$), their results are consistent with Bogoliubov approximation.

In the lower panel (b) of Fig. 2 we show the amplitude of the oscillations $\Delta n_{ex}/n$ as function of a_f. They are calculated by averaging the values of different oscillations in the large-time regime where the amplitude does not change appreciably, and their uncertainty is the standard deviation between them. For $a_f \lesssim 1000a_0$, they exhibit a cubic decay as we go to smaller scattering lengths. For $a_f \gtrsim 1000a_0$, the average of the oscillations approaches $\bar{n}_{ex}/n = 1$ and therefore its amplitude starts to slowly decrease. We conclude that whether the gas is in the weakly interacting regime or not, the oscillatory behaviour is always present. However, far from the resonance, as the energy of the molecular state becomes very large, the oscillations become very rapid and their amplitude quickly goes to zero.

In [7] it was found that in quenches to large scattering lengths ($a_f \geq 300a_0$) in an ultracold ^{39}K atomic gas, three-body processes are not relevant in the first $50\mu s$ after the quench. Since $50/|E_B| \simeq 41\mu s$ for $a_f = 700a_0$, we expect the oscillations to be measured.

B. Tan's contact

The momentum distribution of a quantum gas governed by a two-body, s-wave contact interaction always decays as $1/k^4$ for large momenta [8]. The Tan's contact is defined as

$$C(t) = \lim_{\mathbf{k}\to\infty} \mathbf{k}^4 n_{\mathbf{k}}\,, \tag{III.5}$$

and it physically represents the strength of two-body, short range correlations. In Bogoliubov theory this limit takes the value $C_0 = 16\pi^2 a^2 n^2$.

In Fig. 3 we plot $C(t)$ for several quenches of a non-interacting gas to different scattering lengths $a_f > 0$. The inset shows the $1/k^4$ tail of the momentum distribution of the gas a certain time after the quench in the case of $a_f = 700a_0$. The Tan's contact also exhibit coherent oscillations due to a virtual transfer of pairs of atoms to the molecular bound state, which as we will see have a constant period of $T = 2\pi/|E_B|$ for $a_f \lesssim 1000a_0$.

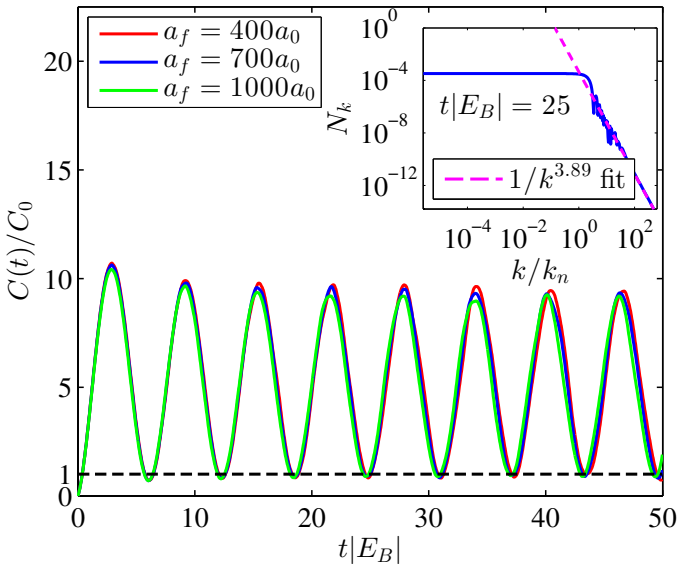

FIG. 3. Tan's contact $C(t)$ for quenches from $a_i = 0$ to $a_f > 0$ as function of time. The plot is rescaled in units of the Bogoliubov contact C_0 and the energy of the molecular bound state $|E_B|$. Inset: momentum distribution after a certain time in a quench from non-interacting to $a_f = 700a_0$.

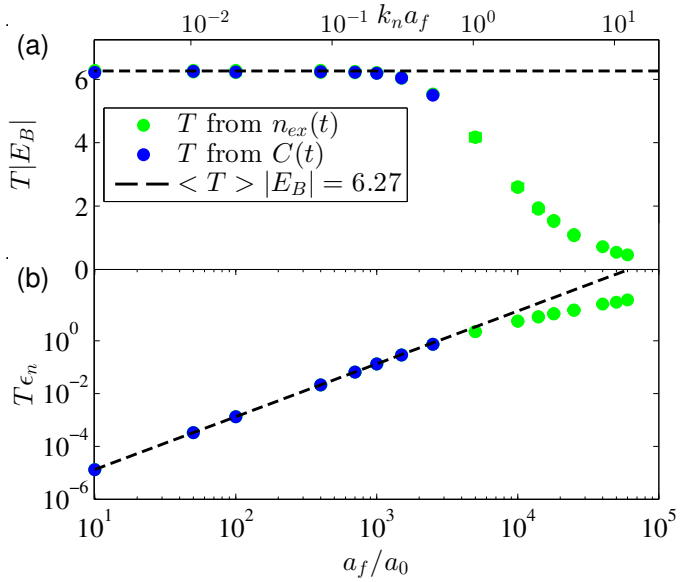

FIG. 4. **(a)** Period T (in units of $|E_B|$) of the oscillations of $n_{ex}(t)/n$ and $C(t)$ after the quench as function of a_f. **(b)** The same in units of ϵ_n.

N.B. that Bogoliubov C_0 remains as a lower limit for the variational $C(t)$.

This contrasts with the results of [18], where coherent atom-molecule oscillations are not present in the Tan's contact and a time-independent contact is found.

C. Period of the coherent oscillations as function of the final scattering length

In Fig. 4 we plot the period T of the oscillations of the non-condensed fraction and the Tan's contact after an instantaneous quench to different values of the scattering length a_f. The periods are obtained using fits to extrapolate the values calculated for finite Λ and M to $\Lambda \to \infty$ and $M \to \infty$ (see App. B). The corresponding errors are given by the fit. As shown in the figure, both periods exhibit a good agreement in the range where the ones of $C(t)$ were calculated.

In the top panel (a), we observe that below $a_f \simeq 1000a_0$ the period has a constant value of $T = 2\pi/|E_B|$ independently of a_f. For larger scattering lengths, the value of the period starts decreasing. In the bottom panel (b), for $a_f \gtrsim 1000a_0$, T approaches a new universal value in units of ϵ_n, anticipating a crossover to the unitary regime. However, because accessing larger values of the interaction requires more computational power, we are only able to anticipate the crossover, not completely seeing the new constant value of T.

D. Universal prethermal dynamics

In this section we study the dynamics of the population of individual $\mathbf{k}$ states after instantaneous quenches from a non-interacting BEC to the strongly interacting regime. The population $\tilde{N}_{\mathbf{k}}(t) = (N_{\mathbf{k}}(t)/n_{ex}(t))k_n^3$ is rescaled in the same manner as in [3], and we find an universal behaviour in units of k_n and t_n above a certain value of a_f, indicating the consistency of our results with the unitary regime.

In Fig. 5 we see that, after the quench, $\tilde{N}_{\mathbf{k}}(t)$ rapidly grows, exhibiting coherent oscillations that have a maximum and later saturate to a steady state. In [3], a sigmoid fit is employed to calculate the value of the population in the steady state and the initial growing time. This can only work with lots of difficulties for our data at small momenta, due to the oscillations, while at large momenta the first oscillation is much larger than the steady state and a sigmoid fit is definitely not the correct tool to extract those parameters. Therefore we have used another criterium to calculate the initial growing time τ_{grow} and the rescaled population of the steady state $\tilde{N}_{std}$. We get the position of the global maximum and calculate the time at which $\tilde{N}_{\mathbf{k}}(t)$ reaches 1/4 of its value; this will be the time of growth τ_{grow}. For the steady state $\tilde{N}_{std}$, we just calculate the average value of the last oscillations.

As shown in the top panel (a) of Fig. 6, the time of growth τ_{grow}/t_n as function of the momentum k/k_n of the level, rescaled in units of the Fermi time and momentum, exhibits a crossover from a $1/k$ decay for $k << k_n$ to a $1/k^2$ decay for $k >> k_n$, as measured in [3]. This reminds us of the shape of Bogoliubov quasiparticle

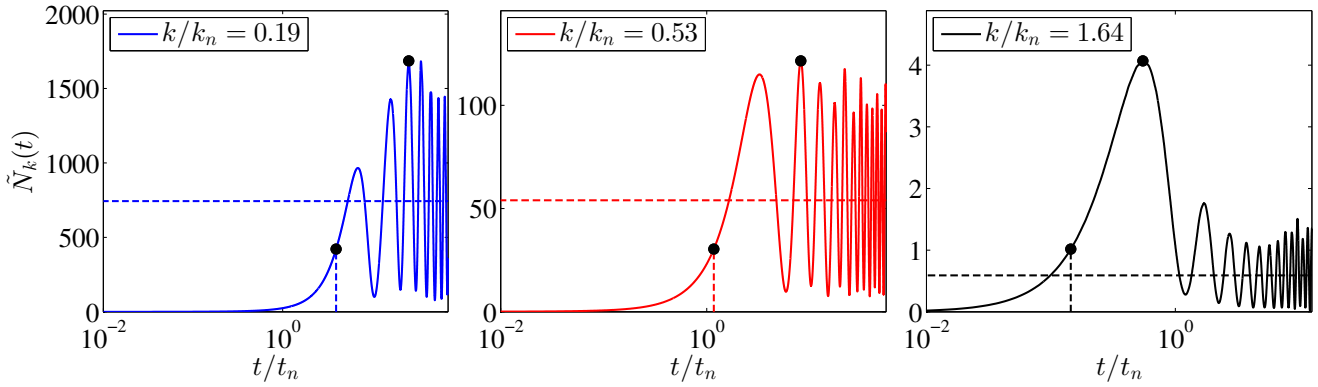

FIG. 5. Dynamics of the population of an excited state $\tilde{N}_{\mathbf{k}}$ in a condensate of density $n = 10^{12} cm^{-3}$ after a quench from $a_i = 0$ to $a_f = 20000a_0$ (solid line). The coherent oscillations are present during all the dynamics. The dashed horizontal line corresponds to the average value of the oscillations in the steady state reached at large times after the quench $\tilde{N}_{std}$. The dashed vertical line is the time of growth of the number of particles with momentum k (τ_{grow}/t_n), which has been taken to be the time at which $\tilde{N}_k$ reaches 1/4 of its maximum value (both signalised by black dots).

spectrum, where excitations are phonons for $k\xi << 1$ and particle-like for $k\xi >> 1$; only that at unitarity the natural time and length scales are the Fermi time t_n and the inverse of the Fermi momentum k_n. The fact that we are able to reproduce the results of [3] implies that this behaviour of the time of growth is completely due to lossless, two-body dynamics, that are taken into account in our model. However, in the experiment, oscillations, if present, are damped. This may be due to Beliaev and Landau scattering, which are neglected in our model and induce a loss of atom-molecule coherence that very likely will damp the oscillations.

The bottom panel (b) of Fig. 6 shows the average population of the large-time steady state of the oscillations $\tilde{N}_{std}$ as function of the momentum of the level k/k_n, rescaled in units of the Fermi momentum. Rather than the exponetial decay measured in [3], our calculation shows the typical $1/k^4$ decay for a quantum gas interacting via a two-body, s-wave contact interaction. It is therefore logical that our model cannot predict such an exponential decay. The explanation of this behaviour remains as a theoretical challenge.

IV. CONCLUSIONS

In this Master's thesis we have employed the NSJ variational formalism to study the dynamics of a homogeneous, degenerate Bose gas after instantaneous interaction quenches from the non-interacting regime ($a_i = 0$) to final scattering lengths a_f, ranging from the weakly to the strongly interacting regime. This approach accounts for the coherent excitations of pairs of atoms from the condensate to excited states, as well as for two-body scattering processes between different excited states, but it neglects three- and more-body scattering processes (which is justified in the early-time after the quench as seen in recent experiments), as well as the Beliaev and Landau damping. The presence of a two-atom molecular bound state of energy E_B in the repulsive side of the resonance is also picked including a regularised contact interaction. This induces coherent oscillations after the quench due to a virtual transfer of pairs of atoms to a molecular condensate.

We calculate the equations of motion from the Lagrangian. In the weakly interacting regime, they can be solved analitically and we recover the expressions of the time-dependent Bogoliubov approximation if we use Born approximation. Nevertheless, in general the equations must be solved numerically.

First, we study the oscillatory behaviour of the non-condensed fraction n_{ex}/n. The oscillations are present for every a_f, although their amplitude decreases as a_f^3 for small final scattering lengths ($a_f \lesssim 1000a_0$). After the quench, the average of the oscillations increases up to a large-time steady state. The average population of this steady state increases for larger a_f, slowly approaching $n_{ex}/n = 1$, but never reaching it. The period of the oscillations has a universal (i.e. independent of a_f) value of $T = 2\pi/|E_B|$ for $a_f \lesssim 1000a_0$, while for larger a_f it changes, reaching a new universal value in units of the Fermi energy ϵ_n, and therefore anticipating a crossover to the unitary regime, where $a_f \to \infty$ and the only meaningful physical scale is the average interparticle distance $n^{-1/3}$.

The Tan's contact $C(t)$ also exhibits coherent oscillations, and its period agrees perfectly with the one calculated from $n_{ex}(t)/n$ in the range of a_f studied.

Finally, we study the dynamics of the population of individual states with momentum $\mathbf{k}$ after the quench. Rescaling the population of each level $N_{\mathbf{k}}(t)$ with the total density of particles in excited states n_{ex} and the Fermi momentum k_n, it first shows an initial growth in a time τ_{grow}. $\tilde{N}_{\mathbf{k}}(t) = (N_{\mathbf{k}}(t)/n_{ex}(t))k_n^3$ also exhibits coherent oscillations, although we discern a large-time

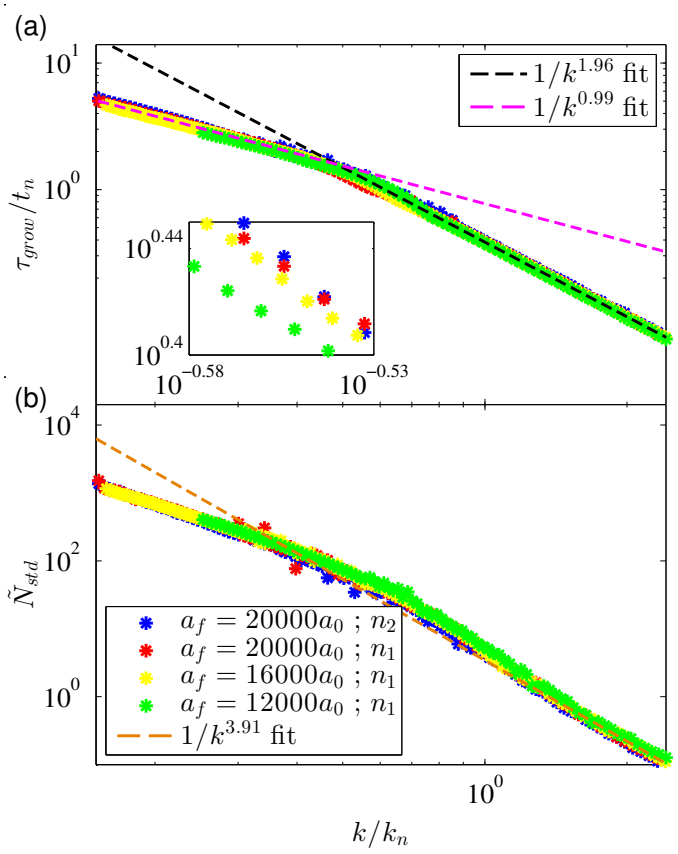

FIG. 6. **(a)** Time of growth τ_{grow}/t_n of $\tilde{N}_k$ as function of k/k_n after a quench to the strongly interacting regime, for several values of a_f and densities $n_1 = 1 \cdot 10^{12} cm^{-3}$ and $n_2 = 5 \cdot 10^{12} cm^{-3}$. For $a_f \gtrsim 16000a_0$, as can be regarded in the inset, all data falls into the same curve independently of the values of a_f and n, indicating the universal behaviour of the unitary regime. **(b)** Average population of the steady state of the oscillations $\tilde{N}_{std}$ reached after a quench to the strongly interacting regime as function of k/k_n. The fit shows the $1/k^4$ decay expected for a quantum gas with a two-body, s-wave contact interaction.

steady state in the average of the oscillations $\tilde{N}_{std}$.

We find that τ_{grow} experiences a crossover from a $1/k$ decay for $k << k_n$ to a $1/k^2$ decay for $k >> k_n$, as it was measured in [3], even though in this work they use a sigmoid fit to calculate the initial time of growth of the population. Thus, this behaviour must be a consequence of lossless, two-body dynamics that is taken into account in our model. However, coherent oscillations, if present in the experiment, are damped. This may be due to Beliaev and Landau decays, that produce a loss of atom-molecule coherence and are not present in our model.

As for the large-time steady state in the average of oscillations, $\tilde{N}_{std}$ decays with a $1/k^4$ tale. We therefore are not able to see the exponential decay measured in [3], but this should not be surprising since we consider a gas with a two-body, s-wave contact interaction.

In future work, it will be interesting to account for Beliaev and Landau collisions, expanding our ansatz to include these terms, and see how they affect the coherent oscillations and the $1/k^4$ decay of the momentum distribution.

V. PERSPECTIVES

A. Dynamics of correlations in strongly interacting Bose gases

For a weakly interacting Bose gas, experiments [23] have verified that the excitation spectrum is given with great accuracy by Bogoliubov approximation [20]. However, in the strongly interacting regime the shape of the spectrum remains an unaswered question. Beliaev [24] calculated the first corrections to Bogoliubov dispersion using quantum field theory, and already suggested the appearance of a roton minimum similar to that of liquid helium for large enough scattering lengths. In recent experiments [25] [26] indicators of this backbending have been measured in the paricle-like ($k\xi \gg 1$) part of the dispersion.

The shape of the quasiparticle spectrum is reflected in the dynamics of density-density correlations

$$g(\mathbf{r}, \mathbf{r}'; t) = \langle \psi(t) | \hat{\psi}^\dagger(\mathbf{r}) \hat{\psi}(\mathbf{r}) \hat{\psi}^\dagger(\mathbf{r}') \hat{\psi}(\mathbf{r}') | \psi(t) \rangle \ , \quad \text{(V.1)}$$

where the field creation and annihilation operators at a position $\mathbf{r}$ can be written

$$\hat{\psi}^\dagger(\mathbf{r}) = \frac{1}{\sqrt{V}} \sum_{\mathbf{k}} \hat{a}^\dagger_{\mathbf{k}} e^{-i\mathbf{k}\cdot\mathbf{r}} \ , \ \hat{\psi}(\mathbf{r}) = \frac{1}{\sqrt{V}} \sum_{\mathbf{k}} \hat{a}_{\mathbf{k}} e^{i\mathbf{k}\cdot\mathbf{r}} \ . \quad \text{(V.2)}$$

The Fourier transform of $g(\mathbf{r}, \mathbf{r}'; t)$ is the structure factor

$$S(\mathbf{k}, t) = \frac{1}{N} \int d\mathbf{r} d\mathbf{r}' g(\mathbf{r}, \mathbf{r}'; t) e^{-i\mathbf{k}(\mathbf{r}-\mathbf{r}')} \ . \quad \text{(V.3)}$$

For a homogeneous gas, the spatial dependence reduces to $r'' = |\mathbf{r} - \mathbf{r}'| \to r$.

In [16] $g(r, t)$ was calculated after an instantaneous quench from a non-interacting gas to $a_f > 0$ using Bogoliubov theory. For a fixed r, correlations exhibit oscillations for small times and after a last maximum they saturate at some final value for large times. The position of the last maximum as function of time spreads diffusively for $t \ll \tau$ and ballistically for $t \gg \tau$, evidencing a close connection between the dynamics of density-density correlations and the underlying excitation spectrum, as Bogoliubov dispersion exhibits an analogous crossover from a phonon-like regime for $k\xi \ll 1$ to a particle-like one for $k\xi \gg 1$.

Following their idea, we calculate $g(r, t)$ for an instantaneous quench using the variational state (II.8). The structure factor is first obtained from (V.1)-(V.3) to be

$$S(\mathbf{k},t)=\frac{1}{N}\Bigg[\frac{g^*_{\mathbf{k}}(t)}{1-|g_{\mathbf{k}}(t)|^2}Vc_0^2(t)+\frac{|g_{\mathbf{k}}(t)|^2}{1-|g_{\mathbf{k}}(t)|^2}(1+V|c_0(t)|^2)+\frac{1}{1-|g_{\mathbf{k}}(t)|^2}V|c_0(t)|^2+\frac{g_{\mathbf{k}}(t)}{1-|g_{\mathbf{k}}(t)|^2}Vc_0^{*2}(t)$$
$$+\sum_{\mathbf{q}\neq 0}\frac{|g_{\mathbf{k}+\mathbf{q}}(t)|^2}{1-|g_{\mathbf{k}+\mathbf{q}}(t)|^2}\frac{1}{1-|g_{\mathbf{q}}(t)|^2}+2\,\mathrm{Re}\left(\sum_{\mathbf{q}\neq 0}\frac{g^*_{\mathbf{k}+\mathbf{q}}(t)}{1-|g_{\mathbf{k}+\mathbf{q}}(t)|^2}\frac{g_{\mathbf{q}}(t)}{1-|g_{\mathbf{q}}(t)|^2}\right)\Bigg]\,, \quad \text{(V.4)}$$

where the terms of the first line represent correlations between condensed-condensed and condensed-non condensed atoms (i.e., they are also taken into account in Bogoliubov formalism), while those in the second line are correlations between non-condensed-non condensed atoms. N.B. that these last terms are especially hard to calculate due to the dependence on the momentum sums $\mathbf{k}+\mathbf{q}$ of the variational parameters. Now, instead of Λ and M, we have Λ and other three cut-offs related with the number of points in the Gauss-Legendre quadratures of the sums: M_k, M_q and M_θ (with θ being the angle between $\mathbf{k}$ and $\mathbf{q}$). This makes extremely hard to achieve fully-converged results, and therefore here we only present the preliminary, almost-converged results for one quench. The density-density correlations are directly obtained from (V.4) using an inverse Fourier transform. Figure 7(a) shows the non fully-converged $g(r,t)$ as function of time for a fixed r after a quench from non-interacting to $a_f = 4000a_0$. The correlations exhibit the same coherent atom-molecule oscillations as $n_{ex}(t)$ and $C(t)$, but moreover they have an envelope whose shape reminds us of the results of [16] for Bogoliubov theory. The position of the last maximum of the envelope is tracked as function of time and plotted in Figure 7(b). Because the calculation is not fully-converged, we could only access a short regime of time where the shape of the envelope is completely clear. The results obtained with Bogoliubov theory, also displayed in the figure, belong to the diffusive regime at short times and later begin to show a slow crossover towards the ballistic one. The provisional variational results seem to overlap with Bogoliubov prediction for short times and then are renormalised from below. This demonstrates that the dispersion relation at this interaction strength lies below the Bogoliubov spectrum in the particle-like regime, just as measured in [25] and [26], possibly indicating the presence of a precursor of a roton minimum. Nevertheless, these results only allow for a qualitative comparison, since they are not fully-converged. Once this is solved a further analysis is needed to quantitative compare the spreading of correlations with the quasiparticle spectrum.

B. Dynamics of two-component mixtures

It has been predicted [27] that a mixture of bosonic atoms and molecules in which the energy of the latter can be tuned via Feshbach resonance exhibits a quantum phase transition between the atomic superfluid phase (ASF), in which both atoms and molecules are condensed, and a molecular superfluid (MSF), where only molecules are.

It should be possible to apply the Nozières-Saint James variational formalism to study the dynamics of a mixture of two spin components ($\sigma =\uparrow,\downarrow$) that can pair to form molecules. In this case, the Hamiltonian can be written

$$\hat{H}=\sum_{\mathbf{k},\sigma}\epsilon_{\mathbf{k}}\hat{a}^\dagger_{\mathbf{k}\sigma}\hat{a}_{\mathbf{k}\sigma}+\frac{1}{V}\sum_{\mathbf{k},\mathbf{k}',\mathbf{q}}\Bigg[\sum_\sigma\frac{U}{2}\hat{a}^\dagger_{\mathbf{k}\sigma}\hat{a}^\dagger_{\mathbf{q}-\mathbf{k}\sigma}\hat{a}_{\mathbf{q}-\mathbf{k}'\sigma}\hat{a}_{\mathbf{k}'\sigma}$$
$$+g\hat{a}^\dagger_{\mathbf{k}\uparrow}\hat{a}^\dagger_{\mathbf{q}-\mathbf{k}\downarrow}\hat{a}_{\mathbf{q}-\mathbf{k}'\downarrow}\hat{a}_{\mathbf{k}'\uparrow}\Bigg]\,, \quad \text{(V.5)}$$

where the opposite spin interaction g is attractive and can be tuned via Feshbach resonance, while the same spin interaction U is assumed to be weakly repulsive. For simplicity, both are taken to be contact-like.

As a first approximation to this problem, we calculate the phase diagram of a binary mixture in the static situation. The system is assumed to be 2D, as the math is simpler in this case, and therefore in (V.5) V represents the system area. Moreover, we restrict ourselves to the unpolarised situation, where the number of spin-up and spin-down atoms is the same (i.e. $n_\uparrow = n_\downarrow$). In 2D, the renormalisation of the contact interaction between opposite spins

$$-\frac{1}{g}=\sum_{\mathbf{k}}\frac{1}{|E_B|+2\epsilon_{\mathbf{k}}}=\frac{m}{4\pi}\ln\left(\frac{2\epsilon_\Lambda+|E_B|}{|E_B|}\right)\,, \quad \text{(V.6)}$$

introduces a large-energy cut-off $\epsilon_\Lambda = \Lambda^2/(2m)$.

In order to obtain the $T = 0$ phase diagram, we employ a variational approach like in Section II by considering a normalised ground state that also includes pairing between opposite spins (i.e. we want finite expectation values of $\langle\hat{a}^\dagger_{\mathbf{k}\sigma}\hat{a}_{\mathbf{k}\sigma}\rangle$, $\langle\hat{a}_{\mathbf{k}\uparrow}\hat{a}_{-\mathbf{k}\downarrow}\rangle$, $\langle\hat{a}_{\mathbf{k}\sigma}\hat{a}_{-\mathbf{k}\sigma}\rangle$ and $\langle\hat{a}^\dagger_{\mathbf{k}\uparrow}\hat{a}_{\mathbf{k}\downarrow}\rangle$, although the two latter averages vanish in the particular case of an unpolarised gas). With this aim we introduce the transformation

$$\begin{pmatrix}\hat{a}^\dagger_{\mathbf{k}\uparrow}\\ \hat{a}_{\mathbf{k}\downarrow}\end{pmatrix}=\frac{1}{\sqrt{2}}\begin{pmatrix}1&1\\-1&1\end{pmatrix}\begin{pmatrix}\hat{b}^\dagger_{\mathbf{k}a}\\ \hat{b}^\dagger_{\mathbf{k}b}\end{pmatrix}\,, \quad \text{(V.7)}$$

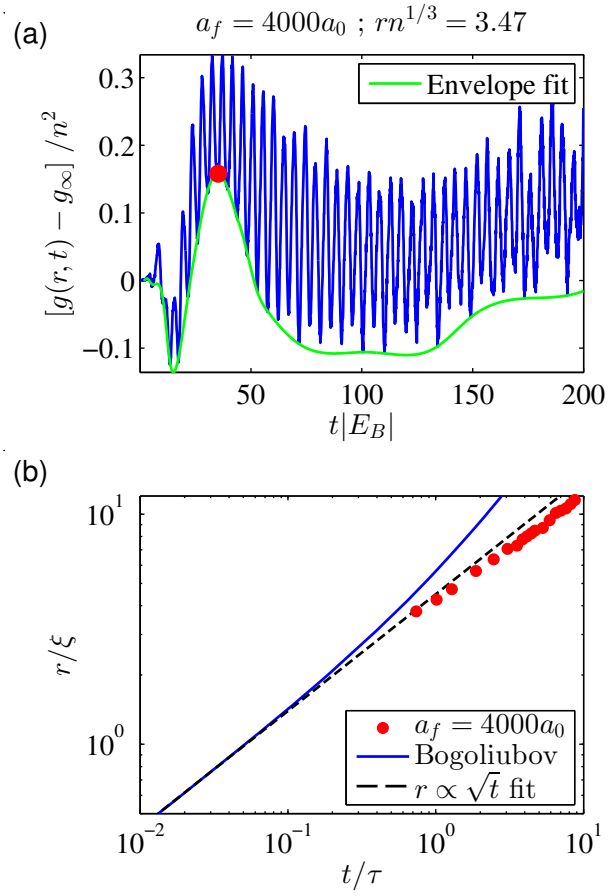

FIG. 7. **(a)** Dynamics of density-density correlations $g(r,t)$ evaluated at a fixed position $rn^{1/3} = 3.47$ for an instantaneous quench from $a_i = 0$ to $a_f = 4000a_0$. Apart from an envelope (green line), whose large-time value g_∞ is used to rescale, they exhibit coherent atom-molecule oscillations. The position of the last maximum of the envelope is marked with a red dot. **(b)** Position of the last maximum of the envelope of the density-density correlations as function of time. The blue line corresponds to Bogoliubov theory; the red dots are our results for a quench to $a_f = 4000a_0$ using the variational formalism.

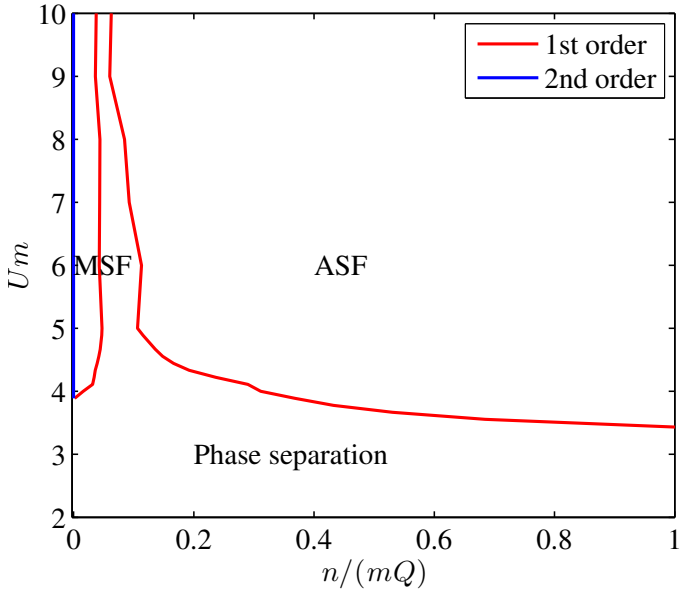

FIG. 8. Static phase diagram of an unpolarised two spin components mixture in 2D. The energies are rescaled in units of $Q = 2|E_B|$. The normal phase is collapsed at $n = 0$.

and then write the variational ground state

$$|\psi\rangle = \frac{1}{\mathcal{A}} \exp\left(\sqrt{V}\sum_{\sigma=\uparrow,\downarrow} c_{0\sigma}\hat{a}^\dagger_{0\sigma} + \sum_{\mathbf{k}}\sum_{\gamma=a,b} \tanh\theta_{\mathbf{k}\gamma}\hat{b}^\dagger_{\mathbf{k}\gamma}\hat{b}^\dagger_{-\mathbf{k}\gamma}\right)|0\rangle \ , \tag{V.8}$$

where $\mathcal{A}$ is the normalisation constant and

$$\tanh 2\theta_{\mathbf{k}\gamma} = \frac{\alpha_\gamma}{\epsilon_{\mathbf{k}} + \beta_\gamma} \tag{V.9}$$

can be written in terms of the variational parameters α_γ and β_γ, that must satisfy $\beta_\gamma > 0$ and $|\alpha_\gamma| \leq \beta_\gamma$.

In order to obtain cut-off independent results, we minimise numerically the expectation value of Hamiltonian (V.5) with a fixed number of particles $\Omega = \langle \hat{H} - \mu\hat{N}\rangle / V$ in the state (V.8) with respect to the three variational parameters $c_0 \equiv c_{0\uparrow} = c_{0\downarrow}$, $\alpha \equiv \alpha_a = -\alpha_b$ and $\beta \equiv \beta_a = \beta_b$ (these equalities come from the fact that we have an unpolarised gas) for different values of the cut-off energy ϵ_Λ. As usually, we then plot the values of Ω obtained as function of ϵ_Λ^{-1} and interpolate to obtain $\Omega(\epsilon_\Lambda^{-1} = 0)$.

The phase diagram as function of U and the density of atoms out of the normal phase n is shown in Figure 8. The normal phase (collapsed at $n = 0$) is characterised by the absence of both atomic ($\chi = |c_0|^2 = 0$) and molecular ($\phi = V^{-1}\sum_{\mathbf{k}} \langle \hat{a}^\dagger_{\mathbf{k}\uparrow}\hat{a}^\dagger_{-\mathbf{k}\downarrow}\rangle = 0$) condensates. For large enough same spin interaction U it can undergo a second order phase transition to the MSF phase, characterised by molecular ($\phi \neq 0$) but not atomic ($\chi = 0$) condensation. The ASF phase, exhibiting both molecular ($\phi \neq 0$) and atomic ($\chi \neq 0$) condensation, is separated by a first order phase transition from the other two.

Appendix A: Shallow quenches

For shallow interaction quenches, $na^3_{i,f} \ll 1$, the dynamics is integrable and one can solve exactly (II.13) and (II.14), recovering the results of Refs. [16, 17]. In this limit, the contribution from $\langle \hat{H}_4\rangle$ (II.12) can be neglected and one can use the Born approximation for the interaction strength $U_{i,f} = 4\pi a_{i,f}/m$. Moreover, one can assume that the condensate depletion is negligible, $|c_0(t)|^2 \simeq n$, and thus the equations of motion can be

simplified to:

$$i\dot{c}_0 \simeq U_f c_0 n \tag{A.1}$$

$$i\dot{g}_{\mathbf{k}} = 2\left[\epsilon_{\mathbf{k}} + 2U_f n\right] g_{\mathbf{k}} + U_f\left(g_{\mathbf{k}}^2 c_0^{*2} + c_0^2\right) . \tag{A.2}$$

It is easy to show that these equations are solved exactly by

$$c_0(t) = \sqrt{n} e^{-iU_f n t} \tag{A.3}$$

$$g_{\mathbf{k}}(t) = \bar{g}_{\mathbf{k}}(t) e^{-2iU_f n t} \tag{A.4}$$

$$\bar{g}_{\mathbf{k}}(t) = \frac{E_{\mathbf{k}f} g_{\mathbf{k}}(0) - i\tan(E_{\mathbf{k}f}t)[U_f n + \xi_{\mathbf{k}f} g_{\mathbf{k}}(0)]}{E_{\mathbf{k}f} + i\tan(E_{\mathbf{k}f}t)[\xi_{\mathbf{k}f} + U_f n g_{\mathbf{k}}(0)]} , \tag{A.5}$$

where $E_{\mathbf{k}f} = \sqrt{\epsilon_{\mathbf{k}}(\epsilon_{\mathbf{k}} + 2U_f n)}$ is the quasiparticle excitation spectrum and $\xi_{\mathbf{k}f} = \epsilon_{\mathbf{k}} + U_f n$. This coincides with the result obtained in Refs. [16, 17] by using a time-dependent Bogoliubov approximation, where one considers the Heisenberg equations of motion for the particle operator $\hat{a}_{\mathbf{k}}(t)$,

$$i\frac{d\hat{a}_{\mathbf{k}}}{dt} = [\hat{a}_{\mathbf{k}}, \sum_{\mathbf{k}} \epsilon_{\mathbf{k}} \hat{a}_{\mathbf{k}}^\dagger \hat{a}_{\mathbf{k}} + \hat{H}_2] .$$

This equation is solved in terms of the Bogoliubov parameters, $\hat{a}_{\mathbf{k}} = u_{\mathbf{k}}(t)\hat{b}_{\mathbf{k}} + v_{\mathbf{k}}^*(t)\hat{b}_{-\mathbf{k}}^\dagger$, where $|u_{\mathbf{k}}(t)|^2 - |v_{\mathbf{k}}(t)|^2 = 1$, giving:

$$i\frac{d}{dt}\begin{pmatrix} u_{\mathbf{k}}(t) \\ v_{\mathbf{k}}(t) \end{pmatrix} = \begin{pmatrix} \xi_{\mathbf{k}f} & U_f n \\ -U_f n & -\xi_{\mathbf{k}f} \end{pmatrix} \begin{pmatrix} u_{\mathbf{k}}(t) \\ v_{\mathbf{k}}(t) \end{pmatrix} .$$

It is easy to show that these coupled equations are solved by

$$\bar{g}_{\mathbf{k}}(t) = \frac{v_{\mathbf{k}}^*(t)}{u_{\mathbf{k}}^*(t)} \qquad |u_{\mathbf{k}}(t)| = \frac{1}{\sqrt{1 - |\bar{g}_{\mathbf{k}}(t)|^2}} , \tag{A.6}$$

and one recovers, e.g. for the density of particles in excited states, the result of [16]

$$n_{ex}^{Bog}(t) = \frac{1}{V}\sum_{\mathbf{k}}\left[\frac{|g_{\mathbf{k}}(0)|^2}{1 - |\bar{g}_{\mathbf{k}}(0)|^2} - U_f(U_i - U_f)n^2 \frac{\epsilon_{\mathbf{k}} \sin^2(E_{\mathbf{k}f}t)}{E_{\mathbf{k}f}^2 E_{\mathbf{k}i}}\right] . \tag{A.7}$$

From the expression above we can perform the same analysis as in Section III D and study the initial growing time τ_{grow} and the steady state in the population of the k-level N_{std}. In this case we obtain the analytical expressions

$$\frac{\tau_{grow}}{\tau} = \frac{\pi}{6}\frac{1}{\sqrt{(k\xi)^2[(k\xi)^2 + 2]}} , \tag{A.8}$$

$$\frac{N_{std}}{n_{ex}}\xi^{-3} = \frac{\sqrt{2^5}\pi}{(k\xi)^2[(k\xi)^2 + 2]} , \tag{A.9}$$

which exhibit the same universal behaviour for $k\xi \ll 1$ and $k\xi \gg 1$ as in Section III D, but in this case in units of ξ and τ instead of k_n and t_n.

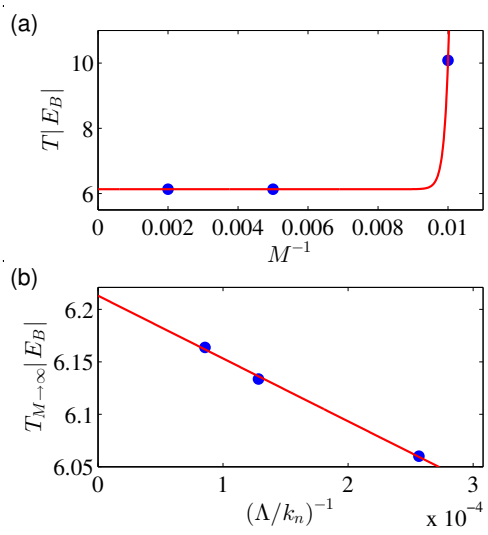

FIG. 9. Two-step extrapolation process of the period of oscillations T of the non-condensed density $n_{ex}(t)$ with respect to the two system regularisation parameters, M and Λ. **(a)** T (blue dots) as a function of M^{-1} for a fixed value of Λ. The $M \to \infty$ value $T_{M\to\infty}$ is extracted via an exponential fit (red solid line). **(b)**: Plot of the extracted period $T_{M\to\infty}$ with respect to Λ^{-1} (blue dots). The extrapolated value $T_{M\to\infty,\Lambda\to\infty}$ is obtained via a linear fit (red solid line).

Appendix B: Convergence of the dynamics

We show here the convergence of our results for the non-condensed density $n_{ex}(t)$ and its oscillation period T with respect to the number of points M on the Gauss-Legendre momentum grid and the momentum cutoff Λ. N.B. that we have followed the same procedure for all data reported in the text. We have found that the dynamics converges exponentially fast with respect to the number of Gauss-Legendre points M used for quadratures, while it only has a linear dependence on the cutoff Λ (at least in the range of Λ computationally accessible). In particular, Fig. 9 shows the dependence of the period of oscillations with respect to both M (panel (a)) and Λ (panel (b)). Once we have extracted $T_{M\to\infty}$ for different values of Λ, we can extract the final value $T_{M\to\infty,\Lambda\to\infty}$ reported in Fig. 4. Our calculations have been limited by a critical slow down of the convergence for both a_f small into the Bogoliubov regime and most importantly for $a_f \to \infty$, making extremely hard to obtain results for $a_f > 60000a_0$ in reasonable times.

Appendix C: Calculation of the steady state in the average of the oscillations of the non-condensed fraction

For every quench in which $a_f > 1000a_0$ we calculate the average of the coherent oscillations $\bar{n}_{ex}/n$ by making the mean value of consecutive maxima and minima. The

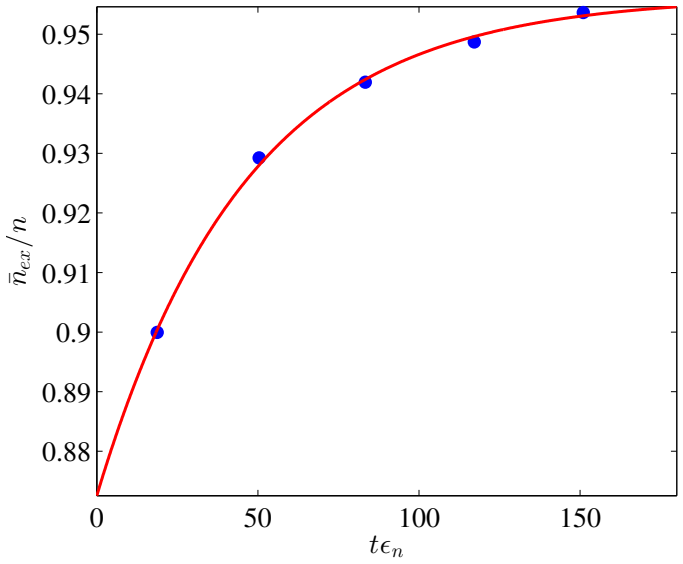

FIG. 10. Fit to obtain the large-time steady-state value of the average of the oscillations ($\bar{n}_{ex}/n$) for a quench between two scattering lengths $a_i = 0$ and $a_f = 60000$ (red line). The blue dots are the values of the average between consecutive maxima and minima, located at their average time.

corresponding time is taken as the mean value of their temporal locations. These are the blue points of Fig. 10, which shows the case of a quench to $a_f = 60000a_0$. To obtain the value of the large-time steady $\bar{n}_{ex}/n$, we use a fit of the form $f(x) = a + be^{cx}$. The uncertainty of $\bar{n}_{ex}/n$ is given by the maximum difference between one oscillation average and the value of the fit for the corresponding time.

For quenches to $a_f \leq 1000a_0$, it would be necessary to calculate n_{ex}/n for larger times in order to see the steady state. Thus we have employed the Bogoliubov theory prediction to obtain an order-of-magnitude estimation to $\bar{n}_{ex}/n$, as explained in the main text.

[1] P. Makotyn, C. E. Klauss, D. L. Goldberger, E. A. Cornell, and D. S. Jin, "Universal dynamics of a degenerate unitary bose gas," *Nature Physics*, vol. 10, pp. 116 EP –, Jan 2014.

[2] C. Eigen, J. A. P. Glidden, R. Lopes, N. Navon, Z. Hadzibabic, and R. P. Smith, "Universal scaling laws in the dynamics of a homogeneous unitary bose gas," *Phys. Rev. Lett.*, vol. 119, p. 250404, Dec 2017.

[3] C. Eigen, J. A. P. Glidden, R. Lopes, E. A. Cornell, R. P. Smith, and Z. Hadzibabic, "Universal Prethermal Dynamics of Bose Gases Quenched to Unitarity," *ArXiv e-prints*, May 2018.

[4] C. Chin, R. Grimm, P. Julienne, and E. Tiesinga, "Feshbach resonances in ultracold gases," *Rev. Mod. Phys.*, vol. 82, pp. 1225–1286, Apr 2010.

[5] W. Zwerger, *The BCS-BEC Crossover and the Unitary Fermi Gas*. Lecture Notes in Physics, Springer Berlin Heidelberg, 2011.

[6] K. Bennemann and J. Ketterson, *Novel Superfluids*. No. v. 2 in International Series of Monographs on Physics, OUP Oxford, 2014.

[7] R. J. Fletcher, R. Lopes, J. Man, N. Navon, R. P. Smith, M. W. Zwierlein, and Z. Hadzibabic, "Two- and three-body contacts in the unitary bose gas," *Science*, vol. 355, no. 6323, pp. 377–380, 2017.

[8] S. Tan, "Energetics of a strongly correlated fermi gas," *Annals of Physics*, vol. 323, no. 12, pp. 2952 – 2970, 2008.

[9] Nozières, P. and Saint James, D., "Particle vs. pair condensation in attractive bose liquids," *J. Phys. France*, vol. 43, no. 7, pp. 1133–1148, 1982.

[10] J. P. Corson and J. L. Bohn, "Bound-state signatures in quenched bose-einstein condensates," *Phys. Rev. A*, vol. 91, p. 013616, Jan 2015.

[11] V. Gurarie and L. Radzihovsky, "Resonantly paired fermionic superfluids," *Annals of Physics*, vol. 322, no. 1, pp. 2 – 119, 2007. January Special Issue 2007.

[12] E. Timmermans, P. Tommasini, R. Côté, M. Hussein, and A. Kerman, "Rarified liquid properties of hybrid atomic-molecular bose-einstein condensates," *Phys. Rev. Lett.*, vol. 83, pp. 2691–2694, Oct 1999.

[13] J. L. Song and F. Zhou, "Ground state properties of cold bosonic atoms at large scattering lengths," *Phys. Rev. Lett.*, vol. 103, p. 025302, Jul 2009.

[14] A. G. Sykes, J. P. Corson, J. P. D'Incao, A. P. Koller, C. H. Greene, A. M. Rey, K. R. A. Hazzard, and J. L. Bohn, "Quenching to unitarity: Quantum dynamics in a three-dimensional bose gas," *Phys. Rev. A*, vol. 89, p. 021601, Feb 2014.

[15] M. Van Regemortel, H. Kurkjian, I. Carusotto, and M. Wouters, "Prethermalization to thermalization crossover in a dilute Bose gas following an interaction ramp," *ArXiv e-prints*, Mar. 2018.

[16] S. S. Natu and E. J. Mueller, "Dynamics of correlations in a dilute bose gas following an interaction quench," *Phys. Rev. A*, vol. 87, p. 053607, May 2013.

[17] C.-L. Hung, V. Gurarie, and C. Chin, "From cosmology to cold atoms: Observation of sakharov oscillations in a quenched atomic superfluid," *Science*, vol. 341, p. 1213, 2013.

[18] X. Yin and L. Radzihovsky, "Postquench dynamics and prethermalization in a resonant bose gas," *Phys. Rev. A*, vol. 93, p. 033653, Mar 2016.

[19] P. Kramer, "A review of the time-dependent variational principle," *Journal of Physics: Conference Series*, vol. 99, no. 1, p. 012009, 2008.

[20] L. Pitaevskii and S. Stringari, *Bose-Einstein Condensation*. International Series of Monographs on Physics, Clarendon Press, 2003.

[21] X. Yin and L. Radzihovsky, "Quench dynamics of a strongly interacting resonant bose gas," *Phys. Rev. A*, vol. 88, p. 063611, Dec 2013.

[22] B. Kain and H. Y. Ling, "Nonequilibrium states of a quenched bose gas," *Phys. Rev. A*, vol. 90, p. 063626, Dec 2014.

[23] J. Steinhauer, R. Ozeri, N. Katz, and N. Davidson, "Excitation spectrum of a bose-einstein condensate," *Phys. Rev. Lett.*, vol. 88, p. 120407, Mar 2002.

[24] S. Beliaev, "Energy spectrum of a non-ideal bose gas," *JETP*, vol. 7, p. 299, 1958.

[25] S. B. Papp, J. M. Pino, R. J. Wild, S. Ronen, C. E. Wieman, D. S. Jin, and E. A. Cornell, "Bragg spectroscopy of a strongly interacting ^{85}Rb bose-einstein condensate," *Phys. Rev. Lett.*, vol. 101, p. 135301, Sep 2008.

[26] R. Lopes, C. Eigen, A. Barker, K. G. H. Viebahn, M. Robert-de Saint-Vincent, N. Navon, Z. Hadzibabic, and R. P. Smith, "Quasiparticle energy in a strongly interacting homogeneous bose-einstein condensate," *Phys. Rev. Lett.*, vol. 118, p. 210401, May 2017.

[27] L. Radzihovsky, J. Park, and P. B. Weichman, "Superfluid transitions in bosonic atom-molecule mixtures near a feshbach resonance," *Phys. Rev. Lett.*, vol. 92, p. 160402, Apr 2004.